

Microscopic theory of photon-induced energy, momentum, and angular momentum transport in nonequilibrium

Yong-Mei Zhang,¹ Tao Zhu,² Zu-Quan Zhang,² and Jian-Sheng Wang²

¹*College of Science, Nanjing University of Aeronautics and Astronautics, Jiangsu 210016, People's Republic of China*

²*Department of Physics, National University of Singapore, Singapore 117551, Republic of Singapore*

(Dated: October 19, 2021)

We set up a general microscopic theory for the transfer of energy, momentum, and angular momentum mediated by photons. Using the nonequilibrium Green's function method, we propose a unified Meir-Wingreen formalism for the energy emitted, force experienced, and torque experienced by the objects due to the emission of photons. Our theory does not require the local thermal equilibrium that is the central assumption of the conventional theory of fluctuational electrodynamics (FE). Moreover, the obtained formulas are valid for arbitrary objects as well as the environment without the requirement of reciprocity. To show the capability of our microscopic theory, we apply the general formulas to transport problems of graphene edges in both equilibrium and nonequilibrium situations. We show the local equilibrium energy radiation of graphene obeys the T^4 law with a converged theoretical emissivity of 2.058%. In the nonequilibrium, we observe nonzero results for force and torque from the edges, which go beyond the predictive ability of the FE theory. Our method is general and efficient for large systems, which paves the way for studying more complex transport phenomena.

Due to fluctuations of the electromagnetic field around bodies, photons transfer energy, momentum, and angular momentum from one object to another or to the environment, which gives rise to abundant physical phenomena such as radiative heat transfer [1, 2], Casimir force [3–5], as well as associated torque [6]. The transport problems of these conserved quantities have attracted tremendous interest for their myriad applications on advanced technologies. For example, the heat transfer in the near field can significantly exceed the black-body limit, which plays an important role in developing alternative techniques such as thermal management [7], energy conversion [8], data storage [9], etc. Photon carrying momentum generates force in both equilibrium and nonequilibrium situations. With certain geometries, Casimir force arises and novel phenomena such as levitation and self-propelling state can be achieved [10, 11]. Angular momentum radiation plays a central role in quantum nanophotonics and topological electrodynamics [12, 13]. Recent studies demonstrate a separation of orbital angular momentum (OAM) and spin angular momentum [14, 15] that have been intensively applied to information and image processings [16–19].

Conventional theories of these transport phenomena are based on fluctuational electrodynamics (FE) of Rytov [20, 21] which combines Maxwell's equations with the local fluctuation-dissipation theorem (FDT) [22]. However, there are several situations that the FE theory might fail. Firstly, FE is a macroscopic theory with usually a phenomenological treatment of materials by a frequency-dependent local dielectric function. This is not sufficient at the subnanometer scale where detailed atomistic modeling of material properties is needed, especially for inhomogeneous materials or near edges [23–25]. Secondly, applying the FDT requires a local thermal equilibrium

for each object that is questionable in real experiments [23]. Furthermore, existing theoretical works only focus on one or two of these phenomena with the usual requirement of reciprocity [26–31]. To the best of our knowledge, a general unified microscopic theory for all three photon-induced transport phenomena is still lacking.

In this letter, using the nonequilibrium Green's function (NEGF) method, we propose a general microscopic formalism for the photon-induced transfer of energy, momentum, and angular momentum in a unified fashion. Combining with the self-energy of the objects, we show that the physical observables of three conserved quantities can be obtained from the corresponding quantum mechanical operators acting on the photon Green's function of the electromagnetic field. The obtained Meir-Wingreen type formulas work for both objects and environment without the assumption of local thermal equilibrium and reciprocity. To demonstrate the power of our microscopic theory, we study the edge effects of transport phenomena of graphene nanoribbons in both equilibrium and nonreciprocal nonequilibrium situations. In particular, we calculate the energy emitted, force experienced, and torque experienced (from OAM radiation) by graphene edges with possible electron transitions due to chemical potential biases. The self-energy is obtained in the eigenmode representation with an efficient velocity matrix method to handle relatively large systems. In thermal equilibrium, we show the edge effects of graphene have an approximate length scale of $t/k_B T$ where t is the hopping parameter and $k_B T$ is the thermal energy at the temperature T . For the bulk two-dimensional system, the heat emission of graphene obeys the T^4 law with a converged emissivity of 2.058%, which is in good agreement with the value implied by the Dirac model [32]. Moreover, we demonstrate nonzero momentum and an-

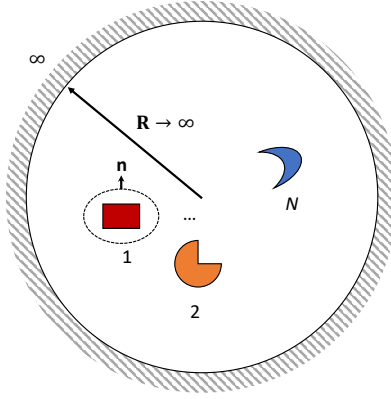


FIG. 1. Schematic setup of N objects in vacuum with arbitrary geometry and the environment served as bath at infinity.

angular momentum radiations in the nonequilibrium situation in which the FE theory does not apply.

To tackle the fluctuating electromagnetic field around bodies, we explore the NEGF method [33, 34] as our basic tool. The fundamental quantity of interest is the photon Green's function defined by the vector potential A_μ as,

$$D_{\mu\nu}(\mathbf{r}, \tau; \mathbf{r}', \tau') = \frac{1}{i\hbar} \langle T_\tau A_\mu(\mathbf{r}, \tau) A_\nu(\mathbf{r}', \tau') \rangle. \quad (1)$$

Here τ, τ' are Keldysh contour times, \mathbf{r}, \mathbf{r}' are the positions, T_τ is the contour-order operator, μ and ν take x, y, z directions. From the contour Green's function, we can determine the lesser ($<$), greater ($>$), retarded (r), and advanced (a) Green's functions in the usual way [35]. For convenience, we adopt the $\phi = 0$ gauge [36] with electric field strength $\mathbf{E} = -\partial\mathbf{A}/\partial t$, and magnetic induction by $\mathbf{B} = \nabla \times \mathbf{A}$. A perturbation theory with the $-\mathbf{j} \cdot \mathbf{A}$ interaction, where \mathbf{j} is the electric current density, leads to a Dyson equation $D = v + v\Pi D$, with $v^{-1} = \epsilon_0(\omega^2 - c^2\nabla \times \nabla \times \cdot)$ as a differential operator acting on D in frequency domain, c is the speed of light, and the self-energy Π is the lowest order current-current correlation function in the random phase approximation.

Now, we consider N physical objects with arbitrary geometry in vacuum. The environment is represented by a sphere of “bath-at-infinity” with radius $\mathbf{R} \rightarrow \infty$ as depicted in Fig. 1. The major physical observables of energy, momentum, and angular momentum transport are the heat emitted, radiation resultant force, and torque applied to each of the N objects, respectively. We calculate these observables by surface integration of the corresponding fluxes with an outward norm. Using the divergence theorem, the surface integrals can be transformed into volume integrals over the object. Then, we have the net energy emission I_α , the total force experienced \mathbf{F}_α ,

and the total torque experienced \mathbf{N}_α , for object α :

$$\begin{pmatrix} I_\alpha \\ \mathbf{F}_\alpha \\ \mathbf{N}_\alpha \end{pmatrix} = \oint_{\Sigma} \begin{pmatrix} \mathbf{S} \\ \mathbf{T} \\ \mathbf{r} \times \mathbf{T} \end{pmatrix} \cdot d\mathbf{\Sigma} = \int_V \begin{pmatrix} -\mathbf{E} \cdot \mathbf{j} \\ \mathbf{f} \\ \mathbf{r} \times \mathbf{f} \end{pmatrix} dV, \quad (2)$$

where $d\mathbf{\Sigma}$ is the surface element with outward norm, dV is the volume element, $\mathbf{S} = (\mathbf{E} \times \mathbf{B})/\mu_0$ is the Poynting vector, $\mathbf{T} = \epsilon_0\mathbf{E}\mathbf{E} + \frac{1}{\mu_0}\mathbf{B}\mathbf{B} - u\mathbf{U}$ is the Maxwell stress tensor with $u = \frac{1}{2}(\epsilon_0 E^2 + B^2/\mu_0)$, \mathbf{U} is the identity, and $\mathbf{f} = \rho\mathbf{E} + \mathbf{j} \times \mathbf{B}$ is the Lorentz force density. Since charge and current densities are related by the continuity equation $\partial\rho/\partial t = -\nabla \cdot \mathbf{j}$, in steady state, we can perform integration by parts in time as well as in space (namely, $\langle ab \rangle = -\langle \dot{a}b \rangle$, $\int dV a \partial_\mu b = -\int dV (\partial_\mu a) b$), transforming the force density as $\mathbf{f} = \sum_\nu j_\nu \nabla A_\nu$.

In performing the quantum-mechanical steady state average, we use a symmetric order of the operators $\langle AB + BA \rangle/2 = i\hbar \int_0^\infty \frac{d\omega}{2\pi} G_{AB}^K(\omega)$, where the Keldysh Green's function is $G_K^K = G^< + G^>$ with $G_{AB}^<(t - t') = \langle B(t')A(t) \rangle/(i\hbar)$ and $G_{AB}^>(t - t') = \langle A(t)B(t') \rangle/(i\hbar)$. To conveniently manipulate the expression, we introduce an intermediate quantity

$$F_{\mu\nu}(\mathbf{r}, \tau; \mathbf{r}', \tau') = \frac{1}{i\hbar} \langle T_\tau A_\mu(\mathbf{r}, \tau) j_\nu(\mathbf{r}', \tau') \rangle. \quad (3)$$

Then, the current density \mathbf{j} connects back to the vector field \mathbf{A} by evoking the linear response, $\mathbf{j} = -\Pi_\alpha \mathbf{A}$ on the contour. Since the $\langle AA \rangle$ correlation gives the Green's function D , after applying the Langreth rule [37] to $D\Pi_\alpha$ defined on contour, we can express the three observables in terms of F , by taking time or spatial derivatives [35].

Finally, we obtain our central results that are the following Meir-Wingreen type formulas for I_α , \mathbf{F}_α , and \mathbf{N}_α :

$$\begin{pmatrix} I_\alpha \\ \mathbf{F}_\alpha \\ \mathbf{N}_\alpha \end{pmatrix} = \int_0^\infty \frac{d\omega}{2\pi} \Re \text{Tr} \left[\begin{pmatrix} -\hbar\omega \\ \hat{\mathbf{p}} \\ \hat{\mathbf{L}} \end{pmatrix} (D^r \Pi_\alpha^K + D^K \Pi_\alpha^a) \right]. \quad (4)$$

In the above, $\hbar\omega$ is obtained from energy operator $i\hbar\partial/\partial t$ acting on Fourier transform of D ; $\hat{\mathbf{p}} = -i\hbar\nabla$ is the momentum operator acting on the first spatial argument of D ; $\hat{\mathbf{L}} = \mathbf{r} \times \hat{\mathbf{p}} + \hat{\mathbf{S}}$ is the angular momentum operator with the spin operator $S_{\nu\gamma}^\mu = (-i\hbar)\epsilon_{\mu\nu\gamma}$ acting on the directional index space of D . $\epsilon_{\mu\nu\gamma}$ is the Levi-Civita symbol. The trace is over the space \mathbf{r} as a volume integral and summation over the index μ . The symbol \Re stands for the real part. The lesser (greater) Green's function is related to the retarded/advanced ones with the Keldysh equation, $D^{<(>)} = D^r \Pi^{<(>)} D^a$, here $\Pi^{<(>)}$ is the total self-energy summed over α , i.e. $\Pi^{<(>)} = \sum_\alpha \Pi_\alpha^{<(>)}$. In a tight-binding model, if we use an electron system with the electron-photon coupling matrix $M_{jk}^{l\mu}$ for the unit cell l with j, k being electron sites, the self-energy from each object, serving also as bath for photons, is given by

$$\Pi_\alpha^{l\mu, l'\nu}(\tau, \tau') = -i\hbar \text{Tr}_e [M^{l\mu} G(\tau, \tau') M^{l'\nu} G(\tau', \tau)], \quad (5)$$

where G is the electron Green's function of object α , and the trace is over the electron sites. We note that the retarded self-energy is related to the dielectric function by $\Pi^r = -\epsilon_0\omega^2(\epsilon - 1)$, which in turn can be related to electric conductivity of materials [38].

Another advancement of the Meir-Wingreen formula Eq. (4) is that they also works for the environment ($\alpha = \infty$) where the trace operation is interpreted as an integration over the sphere and sum over the direction index. The self-energy for the bath at infinity can be worked out by conservation laws of the three kinds of transport quantities for $\alpha = 1, 2, \dots, N$ and ∞ as a whole. This requirement demands $\Pi_\infty^r = -v^{-1}$. Alternatively, a dust model integrating over the space $|\mathbf{r}| > R$ can be built by considering a one-dimensional chain model with a finite central region and consider the effect of non-reflecting boundary conditions [39]. Finally, one matches the surface integral results of the Poynting vector and Maxwell stress tensor. They all lead to an expression

$$\Pi_\infty^r = -i\epsilon_0 c \omega \left(\mathbf{U} - \hat{\mathbf{R}} \hat{\mathbf{R}} \right), \quad (6)$$

here the retarded self-energy is expressed in dyadic notation, $\hat{\mathbf{R}} = \mathbf{R}/R$ is the unit vector pointing from the coordinate origin to a point on the sphere. If the only source of the field is the bath at infinity, using the Keldysh equation, one can verify that the energy density is precisely given by the Planck formula, as one should expect [35]. However, there is one special case that the Meir-Wingreen formula at $\alpha = \infty$ fails — the emission of angular momentum to infinity. The expression from the Meir-Wingreen formula differ by a factor of 2, in comparison to the surface integral result, which is $N_\infty = \int_0^\infty \frac{d\omega}{\pi} \text{Tr}[\mathbf{R} \hat{\mathbf{p}} \times \Pi_\infty^a D^<]$ where $\Pi_\infty^a = (\Pi_\infty^r)^\dagger$ [40], here $\mathbf{R} \hat{\mathbf{p}}$ is a dyadic cross-product with another dyadic, and the trace is to sum over the directional indices and integrating over the solid angle multiplied by R^2 . We suspect that this is due to the extra \mathbf{r} in angular momentum, probing higher order effects in Green's functions.

Here, we apply the general theory to the system of graphene nanoribbon. In particular, we study the non-reciprocal edge effects in the nonequilibrium situation in which the conventional FE theory fails. Further approximations are needed for a concrete calculation. Firstly, we make a multipole expansion, $D^r(\mathbf{R}, \mathbf{r}) = D^r(\mathbf{R}, \mathbf{0}) + \mathbf{r} \cdot \partial D^r(\mathbf{R}, \mathbf{r}')/\partial \mathbf{r}'|_{\mathbf{r}'=0} + \dots$, and keep the lowest non-vanishing order as the monopole term for force is identically zero. Secondly, the graphene ribbon is lattice periodic in x -direction, so the self-energy can be calculated in the eigenmode representation which is more efficient than that of frequency integration [40]. After performing the integration of solid angle and frequency, we obtain the formula of energy emitted as

$$I = \frac{4\alpha}{3\hbar c^2} \sum_{\mu, nn'} (\epsilon_n - \epsilon_{n'})^2 \Theta(\epsilon_n - \epsilon_{n'}) |\langle n | V^\mu | n' \rangle|^2 \times f_n(1 - f_{n'}), \quad (7)$$

where $\alpha \approx 1/137$ is the fine structure constant, ϵ_n is the energy of state n with the Fermi distribution function $f_n = 1/(e^{\beta_{L(R)}(\epsilon_n - \mu_{L(R)})} + 1)$ where $\beta_{L(R)} = 1/k_B T_{L(R)}$ and $\mu_{L(R)}$ is the chemical potential applied to the left (right) lead. Taking left or right chemical potential in the Fermi function is determined by the sign of group velocity which is calculated by $\langle n | V^\mu | n \rangle$ [41], V^μ is the component of velocity matrix in the μ -direction. This treatment realizes a nonequilibrium situation in a ballistic system. $\Theta(x)$ is the step function which is 1 for $x > 0$ and 0 otherwise. This formula can also be obtained from the Fermi golden rule or the Boltzmann transport theory [42]. Similarly, we can derive the formula for torque as

$$N_z = \frac{4\alpha}{3c^2} \sum_{nn'} (\epsilon_n - \epsilon_{n'}) \Theta(\epsilon_n - \epsilon_{n'}) \Im \left\{ \sum_{nn'} f_n(1 - f_{n'}) \times \left[\langle n | V^x | n' \rangle \langle n' | V^y | n \rangle - \langle n | V^y | n' \rangle \langle n' | V^x | n \rangle \right] \right\}, \quad (8)$$

which agrees to the formula obtained in real space [40].

The situation for force is a bit more complex that a concrete formula has not yet been given. Here, we introduce a notation $eU_\gamma^\mu \equiv \sum_l M^{l\mu} r_\gamma^l$ where U_γ^μ has two indices of direction x, y, z . The superscript index is associated with $M^{l\mu}$ or velocity component and the subscript index is associated with the direction of coordinate r_γ . With some derivations [35], we obtain the force formula

$$F^\mu = \frac{4\alpha}{30\hbar^2 c^4} \sum_{nn'} (\epsilon_n - \epsilon_{n'})^3 \Theta(\epsilon_n - \epsilon_{n'}) f_n(1 - f_{n'}) \times \text{Tr} \left[4 \sum_\nu (\rho_n U_\nu^\mu \rho_{n'} V^\nu - \rho_n V^\nu \rho_{n'} U_\mu^\nu) - \sum_\nu (\rho_n U_\nu^\mu \rho_{n'} V^\nu - \rho_n V^\mu \rho_{n'} U_\nu^\nu) - \sum_\nu (\rho_n U_\nu^\nu \rho_{n'} V^\mu - \rho_n V^\nu \rho_{n'} U_\nu^\mu) \right], \quad (9)$$

where $\rho_n = |n\rangle \langle n|$ is the density matrix of state n .

Now, we first study the edge effects of the energy emission of graphene nanoribbons in thermal equilibrium. We show in Fig. 2(a) the thermal radiations from graphene nanoribbons with stripe width $M = 700$. As shown, the emission powers from both zigzag and armchair ribbons converge at high temperatures with the T^4 law of gray bodies. The difference between the zigzag and armchair ribbons in the low temperature is because the former is metallic while the latter has a very small bandgap. With the increase in temperature, thermal excitation gradually overcomes the small energy gap, and their difference vanishes. On the other hand, as the edge and bulk contribute differently to the energy emission, we see deviations of the T^4 law for both ribbons at low temperature due to the finite stripe used. This is further supported by the fact that, with $t = 2.8$ eV, the width $M = 700$ is

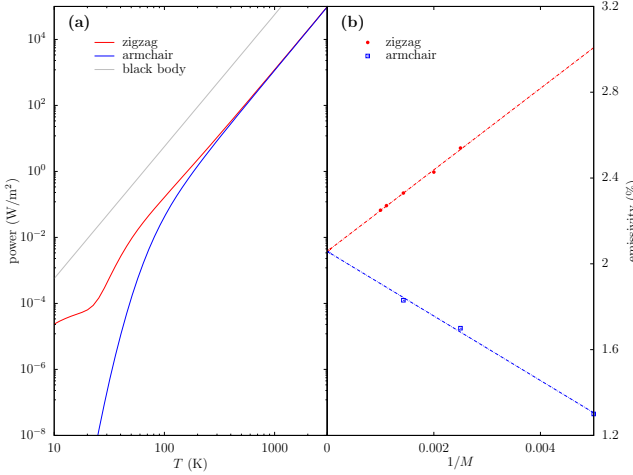


FIG. 2. (a) Temperature dependence of radiation power from zigzag and armchair graphene nanoribbons with width $M = 700$ and $\mu_L = \mu_R = 0$ eV. (b) The calculated emissivity as a function of the inverse of the ribbon width at temperature 300 K. Dash-dotted lines are the best linear fittings of the emissivity, i.e., $2.058 + 189.9(1/M)$ for zigzag ribbon and $2.058 - 150.5(1/M)$ for armchair ribbon.

not much larger than the $t/k_B T \approx 100$ at room temperature. In Fig. 2(b), we check the convergence of the edge effects of the zigzag and armchair ribbons. We found the emissivities of both zigzag and armchair ribbons have an inverse linear relation to the width. For infinitely large width (i.e., $1/M \rightarrow 0$), the emissivity converges to 2.058%, matching almost exactly to the emissivity of 2.056% obtained analytically from integration over all the frequency range of light using the Dirac model [32]. This value is independent of temperature and also agrees with the experimental reports [43] that the thermodynamic emissivity of graphene is smaller than the 2.3% optical emissivity obtained from a circle average of the visible light radiation [44].

According to the FE theory, torque and force are zero for isolated bulk materials [45]. In particular, in local thermal equilibrium, the force is zero due to the reciprocity of Hamiltonian. Thus, we further study the transport phenomena of graphene edge under the nonequilibrium situation in which the FE theory cannot handle. We show in Fig. 3 the calculated power, torque, and force experienced by graphene nanoribbons under different chemical potential biases. Specifically, the chemical potential biases are applied to the x -direction and we compute the torque in the z -direction and force in the x -direction as all other directions generate null results. As shown in Fig. 3, power, torque, and force are significantly changed with μ_L altered from 0 to t , while all remain unchanged for μ_L outside of this range. This is attributed to the concentration of the density of states in this energy window. Interestingly, the energy emis-

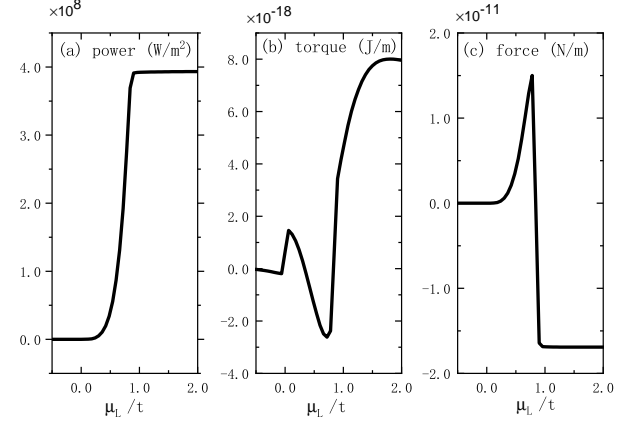


FIG. 3. Photon induced (a) power emission, (b) torque experienced, and (c) force experienced of graphene nanoribbons as functions of left lead chemical potential with $M = 700$ and 401 k -points at the temperature of 300 K. The right lead chemical potential is fixed at $\mu_R = -0.84t$.

sion increases significantly with the increase of μ_L from 0 to t , but the torque and force have more complex features. At certain ranges, the torque and force decrease with increasing μ_L that would due to the cancellation of momentum and angular momentum radiations from transitions between the energy level $E = 0$ to $E = t$ and $E = 0$ to $E = -t$. Such nonvanishing torque and force are edge effects in the nonequilibrium from the chemical potential bias. This feature can be seen more clearly in the density plots in which different results for zigzag and armchair ribbons are shown [35].

In summary, we have proposed a general theory for transport problems of conserved quantities mediated by photons. Using the NEGF method, we derived unified Meir-Wingreen type formulas for the energy emitted, force experienced, and torque experienced of objects (or environment) due to the emission of photons. The theory is general that it does not require local thermal equilibrium and reciprocity of materials. We apply the general theory to the near-edge transport problem of graphene nanoribbons. In the local thermal equilibrium, the energy emission of graphene follows the T^4 law with an emissivity of 2.058% for infinitely wide zigzag and armchair ribbons. Then, we set up a nonequilibrium state in the ballistic regime by putting different chemical potentials based on group velocity in the x -direction. Our results show that nonzero momentum and angular momentum radiations can be generated from the edge in a nonequilibrium situation. There are prominent changes of all three conserved quantities in the bias window $0 < \mu_L < t$, which goes beyond the predictability of the conventional FE theory. Finally, our microscopic theory is general that can be used for more complex systems such as Casimir force in nonequilibrium situations.

Acknowledgments. This work is supported by an MOE tier 2 grant R-144-000-411-112.

SUPPLEMENTARY MATERIALS

A. GREEN'S FUNCTIONS

It is simpler to use a compact notation so that the Green's function defined by Eq. (1) of the main text is a matrix indexed by the space location \mathbf{r} and index μ , as $D(\tau, \tau')$. The contour time is the pair $\tau = (t, \sigma)$ of real time and branch index. Due to the + (forward) and - (backward) branches the contour Green's function gives four Green's functions in real time, $D^{++} = D^t$ is time ordered, $D^{--} = D^{\bar{t}}$ is anti-time ordered, $D^{+-} = D^<$ is lesser, and $D^{-+} = D^>$ is greater. The four are not linearly independent and are constrained by $D^t + D^{\bar{t}} = D^> + D^< = D^K$. The retarded Green's function is $D^r = D^t - D^< = \Theta(D^> - D^<)$ and the advanced is $D^a = D^< - D^{\bar{t}} = -(1 - \Theta)(D^> - D^<)$, such that $D^> - D^< = D^r - D^a$. Let $1 \equiv (\mathbf{r}, \mu, t)$ and $2 \equiv (\mathbf{r}', \nu, t')$, we have the symmetry in time domain as $D^>(1, 2) = D^<(2, 1)$ and $D^r(1, 2) = D^a(2, 1)$. The Fourier transform into frequency is defined by

$$D(\omega) = \int_{-\infty}^{+\infty} dt D(t - t') e^{i\omega(t - t')}. \quad (\text{S1})$$

In frequency domain, we have the Hermitian conjugate $[D^r(\omega)]^\dagger = D^a(\omega)$, $[D^<(\omega)]^\dagger = -D^<(\omega)$. These general relations are also shared by the self-energy Π , since Π is essentially the current-current Green's function. We define reciprocal as being $\Pi^T = \Pi$, here the transpose is in the combined (\mathbf{r}, μ) space.

The contour ordered Dyson equation, $D = v + v\Pi D$, implies the Keldysh equation, $D^< = D^r\Pi^<D^a$, which is valid in general. In global thermal equilibrium, we also have the fluctuation-dissipation theorem, $D^< = N(\omega)(D^r - D^a)$, where $N(\omega) = 1/(e^{\beta\hbar\omega} - 1)$ is the Bose function. A consistency between the two equations, and with the retarded Dyson equation, when the self-energies are additive among the $N + 1$ objects, requires the self-energy for the bath at infinity to be $\Pi_\infty^r = -(v^r)^{-1}$ (actually the argument only determines the difference $\Pi^r - \Pi^a$). This is because the Keldysh equation, defined on a compact domain (central region), together with the fluctuation-dissipation relation, implies,

$$(D^a)^{-1} - (D^r)^{-1} = \sum_{\alpha=1}^{N+1} (\Pi_\alpha^r - \Pi_\alpha^a), \quad (\text{S2})$$

here we name the “object at infinity” as $N + 1$, while the Dyson equation is also

$$(D^r)^{-1} = (v^r)^{-1} - \sum_{\alpha=1}^N \Pi_\alpha^r. \quad (\text{S3})$$

The retarded Dyson equation should be viewed as a differential equation defined on the whole space, and the “bath-at-infinity” is only a no-scattering boundary condition at infinity, thus there is no explicit bath self-energy in the Dyson equation. Taking the Hermitian conjugate and subtracting with the retarded version, and comparing, we find $\Pi_\infty^r - \Pi_\infty^a = (v^a)^{-1} - (v^r)^{-1}$. We can fix it as an equality, $\Pi_\infty^r = -(v^r)^{-1}$, by conservation laws.

B. DERIVATION OF THE MEIR-WINGREEN FORMULAS

We could follow the steps of Krüger *et al.* [10], using $\mathbf{j} = -v^{-1}\mathbf{A}$ to map back to the field \mathbf{A} . Here we use the method outlined in the main text. The advantage of this route is that it is easy to separate out the total contribution from a focused object α . Using our definition of the Green's function $F = \langle A j_\alpha \rangle / (i\hbar)$ and the expression of Joule heating, force, and torque formulas, we obtain

$$I_\alpha = \int_0^\infty \frac{d\omega}{2\pi} \hbar\omega \text{Tr} [F^K(\omega)], \quad (\text{S4})$$

$$\mathbf{F}_\alpha = \int_0^\infty \frac{d\omega}{2\pi} i\hbar \text{Tr} [\nabla_{\mathbf{r}} F^K(\omega)], \quad (\text{S5})$$

$$\mathbf{N}_\alpha = \int_0^\infty \frac{d\omega}{2\pi} \text{Tr} [i\hbar \mathbf{r} \times \nabla_{\mathbf{r}} F^K(\omega) - \hat{\mathbf{S}} F^K(\omega)]. \quad (\text{S6})$$

Here the differentiation with respect to time is $-i\omega$ in frequency domain, and the differential in space is associated with \mathbf{A} , which is the first argument of $F(\mathbf{r}, \mathbf{r}')$. The trace means integration over the whole volume and sum over direction index. $\hat{\mathbf{S}}$ is the spin-1 operator as explained in the main text. This extra spin term is caused by $-\int dV \mathbf{r} \times \partial_\nu (j_\nu \mathbf{A}) = \int dV \mathbf{j} \times \mathbf{A}$, which is a total divergence for force but not for torque.

The next step is to evaluate the Green's function F . One can use the Feynman-diagrammatic method, but here we use a fast argument. The local response of the current due to total field is given by $\mathbf{j} = -\Pi_\alpha \mathbf{A}$, here both the current and field are interpreted as quantum operators, while the contour ordered Green's function Π is just a number. The multiplication is a convolution in \mathbf{r} , τ , and matrix multiplication in index μ . Putting this result into F , and using the fact that the contour ordered Green's function for D and Π are symmetric with respect to the arguments, we obtain $F = -D\Pi_\alpha$. The lesser (greater) component is obtained from the Langreth rule, $-F^{<(>)} = D^r \Pi_\alpha^{<(>)} + D^{<(>)} \Pi_\alpha^a$, which is then our main result in the texts.

As we have defined the three conserved quantities as surface integrals, it is obvious if we sum over the objects from $\alpha = 1, 2, \dots, N$, and $N + 1$, we should get 0. The conservation of energy is obtained from the identity $\text{Tr}(D^>\Pi^< - D^<\Pi^>) = 0$, where $\Pi^{>,<}$ is the total. This identity cannot be used to prove the conservation of total force and torque due to the extra operator in front of D , but the sum is indeed 0 if $\Pi_\infty^a = -(v^a)^{-1}$. This is a consequence of the validity of the Dyson equation. After the summation, the last common factor in Eq. (4) after the various operators is $D^r \Pi^K + D^K \Pi^a = D^r \Pi^K (I + D^a \Pi^a)$, and we have used the Keldysh equation. The extra multiplicative factor $I + D^a \Pi^a$ when equated to 0 is nothing but the Dyson equation of the advanced version, remembering $\Pi^r = \sum_{\alpha=1}^N \Pi_\alpha^r - (v^r)^{-1}$. For equations in frequency domain, the retarded version has $\omega \rightarrow \omega + i\eta$, $\eta \rightarrow 0^+$, and advanced one is obtained by Hermitian conjugate.

C. BATH AT INFINITY

It appears that we have two self-energy expressions for the bath at infinity. One is $-v^{-1}$, and another is Eq. (6). The first one is a differential operator which must act on D in order to see its effect, and the second one is defined on the sphere $|\mathbf{r}| = R$, and is more friendly for actual computation. We demonstrate their consistency with a dust model. We assume for $|\mathbf{r}| \geq R$, the solution for the retarded Green's function is the free one,

$$D_0^r = -\frac{e^{i\frac{\omega}{c}R}}{4\pi\epsilon_0 c^2 R} \left[(\mathbf{U} - \hat{\mathbf{R}}\hat{\mathbf{R}}) + \left(-\frac{1}{i\frac{\omega}{c}R} + \frac{1}{(i\frac{\omega}{c}R)^2} \right) (\mathbf{U} - 3\hat{\mathbf{R}}\hat{\mathbf{R}}) \right]. \quad (\text{S7})$$

A “dust” model is obtained by the replacement, $\omega \rightarrow \omega + i\eta$ in the above solution describing the damping for $|\mathbf{r}| > R$. In evaluating the transport quantities, we need to evaluate the trace of a form $\text{Tr} \hat{O} [D^r \Pi^< D^a \Pi_\infty^a]$. Here \hat{O} is the extra operator acting on D^r , the trace involving the bath at infinity is the volume integral of all space outside the sphere, which we can perform a solid angle integration and $\int_R^\infty dr r^2 \dots$. Since when $\eta = 0$, $v^{-1} D^r = 0$, the effect of the dust is

$$v^{-1} D^r = \epsilon_0 (\omega^2 - (\omega + i\eta)^2) D^r \approx \epsilon_0 (-2i\eta\omega) D^r. \quad (\text{S8})$$

The advanced version is obtained by taking Hermitian conjugate. At asymptotically large distance, we can ignore the second high-order term in $1/R$ and it is sufficient to keep the first term. Then the decay factor is $D^r D^a \propto e^{-2\eta r/c}$. After integrating r from R to infinity, we find a finite result when $\eta \rightarrow 0^+$,

$$\text{Tr} \hat{O} [D^r \Pi^< D^a \Pi_\infty^a] \approx \int d\Omega R^2 \hat{O} [D^r \Pi^< D^a (i\epsilon_0 c\omega)]. \quad (\text{S9})$$

We assume the operator \hat{O} does not mess up the argument in this process. Both D^r and D^a have a transverse projector $\mathbf{U} - \hat{\mathbf{R}}\hat{\mathbf{R}}$ so we also attach this projector to the numerical factor $i\epsilon_0 c\omega$. This gives the surface sphere version of the self-energy for bath at infinity, Eq. (6). We note that this self-energy is local in the solid angle.

As a check of the correctness of the self-energy, we consider a system that consists solely of the bath at infinity and no objects at all. We then evaluate the energy density $u = \frac{1}{2}(\epsilon_0 E^2 + \frac{1}{\mu_0} B^2)$ at the origin, due to the bath at infinity at a temperature T . The thermal average can be expressed in terms of the Green's function, as

$$\langle u \rangle = \int_0^\infty \frac{d\omega}{2\pi} i\hbar \text{Tr}_\mu \left[\epsilon_0 \omega^2 D^< - \frac{1}{\mu_0} \nabla_{\mathbf{r}} \times D^< \times \nabla_{\mathbf{r}'} \right], \quad (\text{S10})$$

here the trace is in direction index, the first gradient operator is over the first argument and second one over the second argument, and after taking the derivatives, the Green's function is evaluated at $\mathbf{r} = \mathbf{r}' = \mathbf{0}$. Applying the

Keldysh equation, $D^< = D^r \Pi_\infty^< D^a$, using the fluctuation-dissipation theorem, $\Pi_\infty^< = N(\omega)(\Pi_\infty^r - \Pi_\infty^a)$, and the expression D_0^r to leading order in $1/R$, performing the trace at the sphere, we obtain

$$\langle u \rangle = \int_0^\infty d\omega \frac{\omega^2}{\pi^2 c^3} \hbar\omega N(\omega), \quad (\text{S11})$$

which is the correct expression for the blackbody radiation.

D. DERIVATION OF POWER, TORQUE AND FORCE FORMULA IN THE EIGENMODE REPRESENTATION

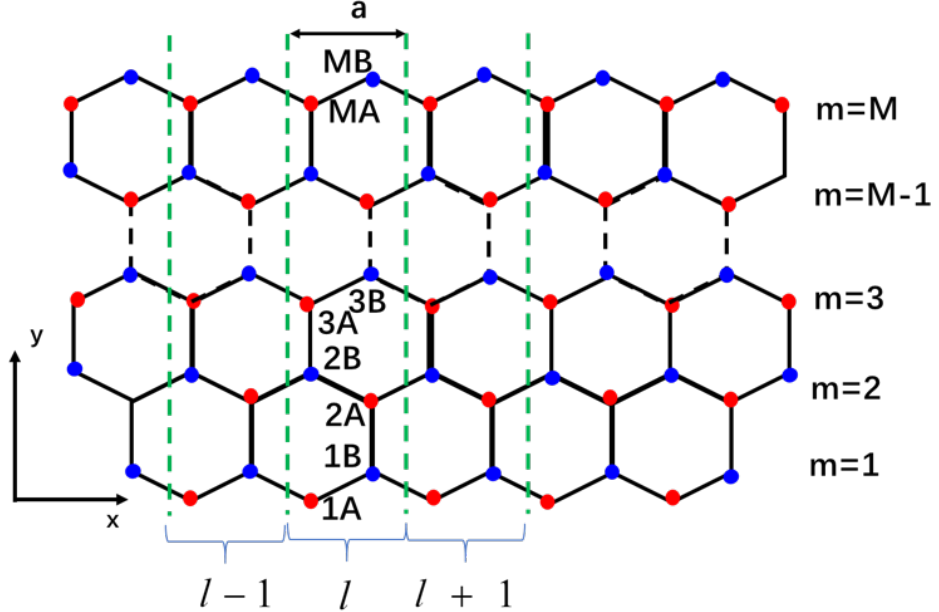


FIG. S1. Graphene nanoribbon with zigzag edge. The x -direction is periodic with unit cells represented by dashed lines and labeled by index l . Each site along y -direction is labeled by index m with two sublattice sites A and B .

In Fig. S1, we show the system of semi-infinite graphene in x - y plane with edges. We further assume that x -direction is periodic so that we can transform the stripe in this direction into k -space. Then, summing over sites becomes integration over k , while keeping the y direction explicitly in real space. We use index l to represent different unit cells in the x -direction, m labels the site of carbon atoms in the y -direction, and z -direction is perpendicular to the graphene plane.

From the main text, the photon's lesser Green's function is defined as

$$D_{\mu\nu}^<(\mathbf{r}', t'; \mathbf{r}, t) = \frac{1}{i\hbar} \langle A_\nu(\mathbf{r}, t) A_\mu(\mathbf{r}', t') \rangle. \quad (\text{S12})$$

Starting from the surface integral Eq. (2) of the main text (or Eq. (4) for the “bath at infinity”, $\alpha = \infty$), we can write the energy emitted as

$$I = \Re \frac{1}{\mu_0} \sum_{\mu, \nu, \gamma, \beta, \varsigma} \epsilon_{\mu\nu\gamma} \epsilon_{\gamma\beta\varsigma} \int d\Omega R^2 \hat{\mathbf{R}}_\mu \int_0^{+\infty} \frac{d\omega}{\pi} \hbar\omega \left(-\frac{\partial}{\partial x'_\beta} \right) D_{\nu\varsigma}^<(\mathbf{r}, \mathbf{r}', \omega) |_{\mathbf{r}'=\mathbf{r}}, \quad (\text{S13})$$

where Ω is the solid angle. Using the Keldysh equation $D_{\mu\nu}^<(\mathbf{r}, \mathbf{r}', \omega) = \sum_{ll', \gamma\varsigma} D_{\mu\gamma}^r(\mathbf{r}, \mathbf{r}_l, \omega) \Pi_{\gamma\varsigma}^{<, ll'}(\omega) D_{\varsigma\nu}^a(\mathbf{r}_{l'}, \mathbf{r}', \omega)$, we have

$$I = \int_0^\infty d\omega \frac{-\hbar\omega^2}{6\pi^2 \epsilon_0 c^3} \Im \sum_{ll', \mu} \Pi_{\mu\mu}^{<, ll'}(\omega), \quad (\text{S14})$$

where \Im takes the imaginary part. Similarly, we can write the angular momentum radiation resultant torque applied to graphene along \hat{z} direction as

$$N_z = \int_0^\infty d\omega \frac{-\hbar\omega}{6\pi^2\varepsilon_0 c^3} \Re [\Pi_{xy}^<(\omega) - \Pi_{yx}^<(\omega)]. \quad (\text{S15})$$

Here $\Pi^<$ is the interacting self-energy summing over all lattice sites. For systems with time reversal symmetry, i.e. the Hamiltonian is real and symmetric, both torque and force are zero in thermal equilibrium. To generate nonzero torque and force, we have to apply a driven potential bias (μ_L, μ_R) to break the symmetry and the system is in nonequilibrium. Moreover, even in nonequilibrium state, the non-zero contribution is only from the edge. We apply a periodic boundary condition in x -direction so that eigenmode can be characterized by traveling waves. The interaction self-energy can be obtained in the eigenmode as

$$\Pi_{\mu\nu}^{<,ll'}(\omega) = -i2\pi \sum_{nn'} \langle n | M^{\nu l'} | n' \rangle \langle n' | M^{\mu l} | n \rangle f_n(1 - f_{n'}) \delta(\varepsilon_n - \varepsilon_{n'} - \hbar\omega), \quad (\text{S16})$$

where n denotes modes with wavevectors k and electron band label, \mathbf{M} is a vector matrix defined by $e\mathbf{V} = \sum_i \mathbf{M}^i$ which can be expressed explicitly in terms of the matrix elements of velocity, $\mathbf{M}_{jk}^i = e(\delta_{ij}\mathbf{V}_{jk} + \delta_{ik}\mathbf{V}_{jk})/2$ where i, j, k are site indices. Substituting Eq. (S16) into Eq. (S14) and Eq. (S15) and performing the frequency integration, we get

$$I = \frac{4\alpha}{3\hbar c^2} \sum_{nn'} (\varepsilon_n - \varepsilon_{n'})^2 \Theta(\varepsilon_n - \varepsilon_{n'}) \sum_\mu |\langle n | V^\mu | n' \rangle|^2 f_n(1 - f_{n'}), \quad (\text{S17})$$

and

$$N_z = \frac{4\alpha}{3c^2} \sum_{nn'} (\varepsilon_n - \varepsilon_{n'}) \Theta(\varepsilon_n - \varepsilon_{n'}) \Im \left\{ \sum_{nn'} f_n(1 - f_{n'}) \left[\langle n | V^x | n' \rangle \langle n' | V^y | n \rangle - \langle n | V^y | n' \rangle \langle n' | V^x | n \rangle \right] \right\}. \quad (\text{S18})$$

These two equations are the main formulas we used to calculate energy and angular momentum radiation. On the other hand, the force acting on an object is due to the emission of momentum out of the object. With the Maxwell stress tensor, the force formula integrating over a large sphere surface is equivalent to an integration of the solid angle, i.e., $\mathbf{F} = \int d\Omega R^2 [\varepsilon_0(\mathbf{R} \cdot \mathbf{E})\mathbf{E} - u\hat{\mathbf{R}}]$. With Eq. (S12) and its Fourier transform in space, we obtain

$$\mathbf{F} = \int_0^\infty \frac{d\omega}{\pi} \int d\Omega R^2 \left[\varepsilon_0(i\hbar\omega^2) \left(D^< \cdot \hat{\mathbf{R}} - \frac{1}{2} \text{Tr}(D^<) \hat{\mathbf{R}} \right) + \frac{i\hbar}{2\mu_0} \text{Tr}(\nabla \times D^< \times \hat{\nabla}) \hat{\mathbf{R}} \right]. \quad (\text{S19})$$

Since the only dependence of angle Ω appears in $\hat{\mathbf{R}}$, integration of an odd number of $\hat{\mathbf{R}}$ produces zero. Thus, we must do a dipole expansion of $D_{\mu\nu}^r(\mathbf{R} - \mathbf{r}_l)$ to have an even order of $\hat{\mathbf{R}}$, i.e. $D_{\mu\nu}^r(\mathbf{R} - \mathbf{r}_l) = D_{\mu\nu}^r(\mathbf{R}) - \mathbf{r}_l \cdot \frac{\partial}{\partial \mathbf{R}} D_{\mu\nu}^r(\mathbf{R}) + \dots$. Substituting it into the Keldysh equation and keeping only the first order term (ignoring the monopole and higher order term), we have

$$D_{\mu\nu}^< = - \sum_{\zeta, \gamma, \xi, l, l'} \left(D_{\mu\xi}^r \Pi_{\zeta\gamma}^{<,ll'} x_\xi^l \partial_\xi D_{\gamma\nu}^a + x_\zeta^l \partial_\zeta D_{\mu\xi}^r \Pi_{\zeta\gamma}^{<,ll'} D_{\gamma\nu}^a \right), \quad (\text{S20})$$

where all the subscript indices mean directions x, y, z . As the retarded photon Green's function is

$$D_{\mu\nu}^r \approx -\frac{e^{-i\frac{\omega}{c}R}}{4\pi\varepsilon_0 c^2 R} (\mathbf{U} - \hat{\mathbf{R}}\hat{\mathbf{R}})_{\mu\nu}, \quad (\text{S21})$$

the Keldysh equation now can be written as

$$D_{\mu\nu}^< = -i\frac{\omega}{c} \left(\frac{1}{4\pi\varepsilon_0 c^2 R} \right)^2 \sum_{\zeta, \gamma, l, l'} \left[(\mathbf{r}_l - \mathbf{r}_{l'}) \cdot \hat{\mathbf{R}} (\mathbf{U} - \hat{\mathbf{R}}\hat{\mathbf{R}})_{\mu\zeta} \Pi_{\zeta\gamma}^{<,ll'} (\mathbf{U} - \hat{\mathbf{R}}\hat{\mathbf{R}})_{\gamma\nu} \right]. \quad (\text{S22})$$

Substituting Eq. (S22) into the force formula Eq. (S19), and integrating over the solid angle, we have

$$F^\mu = \int_0^\infty d\omega \frac{-\hbar\omega^3}{60\varepsilon_0\pi^2 c^5} \sum_{ll'} \left\{ 4\text{Tr}(\Pi^{<,ll'}) (\mathbf{r}_l - \mathbf{r}_{l'})_\mu - \sum_\nu \left[\Pi_{\mu\nu}^{<,ll'} (\mathbf{r}_l - \mathbf{r}_{l'})_\nu + (\mathbf{r}_l - \mathbf{r}_{l'})_\nu \Pi_{\nu\mu}^{<,ll'} \right] \right\}. \quad (\text{S23})$$

With Eq. (S16), we have

$$\sum_{ll'} \Pi_{\mu\nu}^{<,ll'}(\omega) r_\gamma^l = -i2\pi \sum_{nn'} \text{Tr} \left(\sum_l \langle n | M^{\mu l} r_\gamma^l | n' \rangle \sum_{l'} \langle n' | M^{\nu l'} | n \rangle \right) f_n (1 - f_{n'}) \delta(\varepsilon_n - \varepsilon_{n'} - \hbar\omega). \quad (\text{S24})$$

Here, we introduce a notation $eU_\gamma^\mu \equiv \sum_l \mathbf{M}^{\mu l} r_\gamma^l$ where U_γ^μ has two indices of direction x, y, z . The superscript index is associated with $\mathbf{M}^{\mu l}$ or velocity component and the subscript index is associated with direction of the coordinate r_γ . Then we obtain the final formula for the force

$$F^\mu = \frac{4\alpha}{30\hbar^2 c^4} \sum_{nn'} (\varepsilon_n - \varepsilon_{n'})^3 \Theta(\varepsilon_n - \varepsilon_{n'}) f_n (1 - f_{n'}) \text{Tr} \left[4 \sum_\nu (\rho_n U_\mu^\nu \rho_{n'} V^\nu - \rho_n V^\nu \rho_{n'} U_\mu^\nu) \right. \\ \left. - \sum_\nu (\rho_n U_\nu^\mu \rho_{n'} V^\nu - \rho_n V^\mu \rho_{n'} U_\nu^\nu) - \sum_\nu (\rho_n U_\nu^\nu \rho_{n'} V^\mu - \rho_n V^\nu \rho_{n'} U_\nu^\mu) \right], \quad (\text{S25})$$

where $\rho_n = |n\rangle\langle n|$ is the density matrix of state n . For graphene stripe, we find only $F^x \neq 0$ and other component is identically zero. Group velocity of state $|n\rangle$ is calculated by $\langle n | V^x | n \rangle$ which determines the left or right chemical potential used in the Fermi function f_n .

E. VELOCITY MATRIX

Given a Hamiltonian $\hat{H} = C^\dagger H C$ in real space with Hermitian matrix $H_{ij} = H_{ji}^*$ and creation (annihilation) operator C^\dagger (C) of the electrons, the velocity matrix is [40]

$$V_{jk} = \frac{1}{i\hbar} H_{jk} (\mathbf{R}_j - \mathbf{R}_k). \quad (\text{S26})$$

Let $\mathbf{v}_1 = v(0, 1)$, $\mathbf{v}_2 = v(-\sqrt{3}/2, -1/2)$, $\mathbf{v}_3 = v(\sqrt{3}/2, -1/2)$ with $v = a_{cc}t/\hbar$ where $a_{cc} = 0.142$ nm is the bond length between nearest-neighbor carbon atoms in graphene. For zigzag graphene nanoribbon, the velocity operator is

$$V = i\mathbf{v}_1 \left[\sum_{l,m} a_l^\dagger(m+1) b_l(m) \right] - i\mathbf{v}_2 \left[\sum_{l,m=odd} b_l^\dagger(m) a_l(m) + \sum_{l,m=even} b_l^\dagger(m) a_{l-1}(m) \right] \\ + i\mathbf{v}_3 \left[\sum_{l,m=odd} a_l^\dagger(m) b_{l-1}(m) - \sum_{l,m=even} b_l^\dagger(m) a_l(m) \right] + h.c. \quad (\text{S27})$$

Here m represents site as illustrated in Fig. S1, a (a^\dagger) and b (b^\dagger) are annihilation (creation) operators generated by sublattices A and B , respectively. Performing Fourier transform in x -direction with Wakabayashi's convention [46], the velocity can be written as

$$V = i\mathbf{v}_1 \sum_{k_x, m} a_{m+1}^\dagger(k_x) b_m(k_x) - i\mathbf{v}_2 \sum_{k_x, m} \xi b_m^\dagger(k_x) a_m(k_x) + i\mathbf{v}_3 \sum_{k_x, m} \xi a_m^\dagger(k_x) b_m(k_x) + h.c., \quad (\text{S28})$$

where $\xi = e^{-ik_x \tilde{a}/2}$ and $\tilde{a} = \sqrt{3}a_{cc}$ is the lattice constant. Then the velocity matrix can be written as

$$V = \begin{bmatrix} 0 & u \\ u^\dagger & 0 \end{bmatrix}, \quad (\text{S29})$$

and the explicit expression of V^x, V^y can be expressed by u_x and u_y which are given by

$$u^x = \sqrt{3}v \sin \frac{k_x \tilde{a}}{2} \begin{bmatrix} 1 & 0 & 0 & \cdots & 0 \\ 0 & 1 & 0 & \cdots & 0 \\ 0 & 0 & 1 & \cdots & 0 \\ \vdots & \vdots & \vdots & \ddots & \vdots \\ 0 & 0 & 0 & \cdots & 1 \end{bmatrix}, \quad u^y = iv \begin{bmatrix} -g_k/2 & 0 & 0 & \cdots & 0 \\ 1 & -g_k/2 & 0 & \cdots & 0 \\ 0 & 1 & -g_k/2 & \cdots & 0 \\ \vdots & \vdots & \vdots & \ddots & \vdots \\ 0 & 0 & 0 & \cdots & -g_k/2 \end{bmatrix}, \quad (\text{S30})$$

where $g_k = 2 \cos(k_x \tilde{a}/2)$. Similarly, the velocity matrices for armchair graphene are

$$u^x = iv \begin{bmatrix} \xi & -1/2 & 0 & \cdots & 0 \\ -1/2 & \xi & -1/2 & \cdots & 0 \\ 0 & -1/2 & \xi & \cdots & 0 \\ \vdots & \vdots & \vdots & \ddots & \vdots \\ 0 & 0 & 0 & \cdots & \xi \end{bmatrix}, \quad u^y = iv \frac{\sqrt{3}}{2} \begin{bmatrix} 0 & -1 & 0 & \cdots & 0 \\ 1 & 0 & -1 & \cdots & 0 \\ 0 & 1 & 0 & \cdots & 0 \\ \vdots & \vdots & \vdots & \ddots & \vdots \\ 0 & 0 & 0 & \cdots & 0 \end{bmatrix}. \quad (\text{S31})$$

For a stripe with two edges, the angular momenta cancel as the contribution from each edge is equal in magnitude and opposite in sign. To obtain the effect of one edge, in calculation we take a method of sharp cutoff. We separate the graphene nanoribbon into bottom and top parts. The wavefunctions of atoms on the top part are set zero. This is analytically equivalent to set elements of velocity matrices to zero for atoms on the top part.

F. DENSITY PLOT OF RADIATIONS FROM ZIGZAG AND ARMCHAIR EDGES

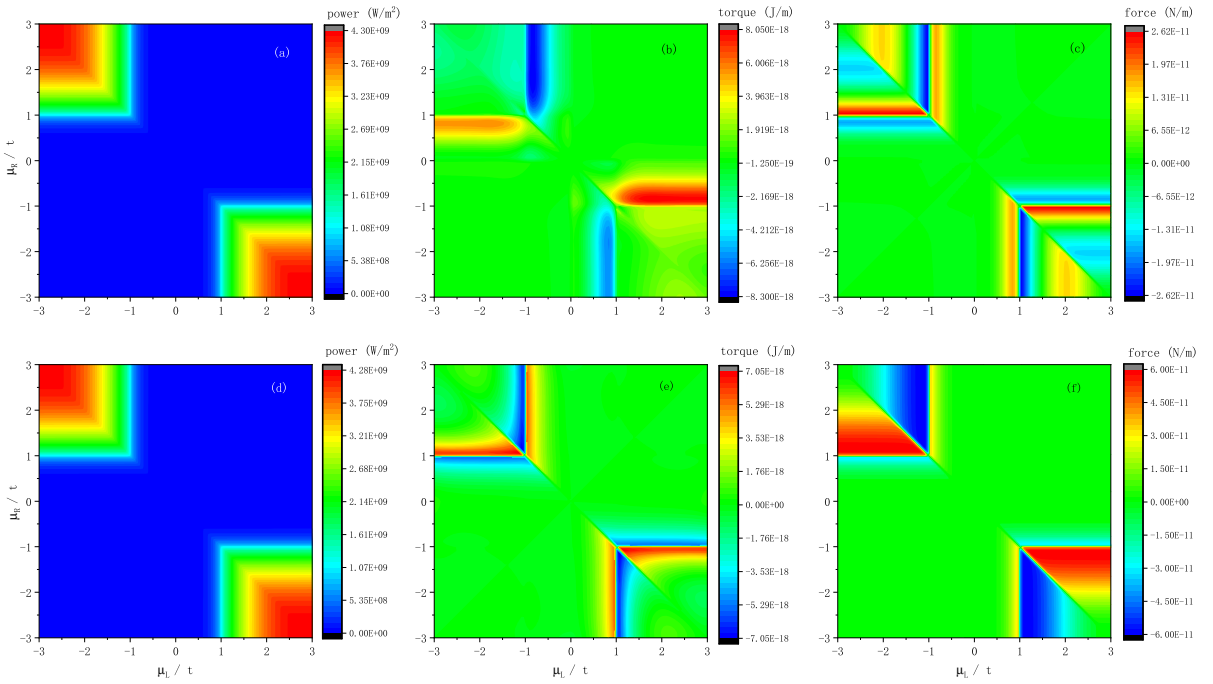


FIG. S2. Intensity of (a) power, (b) torque, and (c) force for zigzag graphene nanoribbon edges with different chemical potentials of left and right leads. (d) - (f) respectively show the same quantities as (a) - (c) but for armchair graphene nanoribbon edges. Other parameters are the same as Fig. 3 of the main text.

The effect of chemical potential can be seen more clearly in the density plot. In Fig. S2, we show energy, torque, and force densities of zigzag and armchair graphene ribbons with potentials μ_L and μ_R . Generally, equal potentials in left and right leads do not generate torque or force. In Fig. S2, stripe patterns can be observed in the top-left corner and bottom-right corner for both zigzag and armchair ribbons. These stripes represent large radiation under different potential bias, corresponding to emission of electrons transmission between the Van Hove singularities at $\pm t$ and zero-energy edge states. As shown in Fig. S2, the energy radiations from zigzag and armchair ribbons are almost identical while the force and torque show very different patterns. This is due to the existence of zero-energy edge states

of zigzag graphene ribbon while for armchair ribbon, resonant transitions occur between the Van Hove singularities. This character demonstrates that the nonzero force and torque radiations are edge effects in nonequilibrium.

[1] A. I. Volokitin and B. N. J. Persson, *Rev. Mod. Phys.* **79**, 1291 (2007).

[2] S.-A. Biehs, R. Messina, P. S. Venkataram, A. W. Rodriguez, J. C. Cuevas, and P. Ben-Abdallah, *Rev. Mod. Phys.* **93**, 025009 (2021).

[3] H. B. G. Casimir, *Proc. K. Ned. Akad. Wet. B* **51**, 793 (1948).

[4] E. M. Lifshitz, *Sov. Phys. JETP* **2**, 73 (1956).

[5] L. M. Woods, D. A. R. Dalvit, A. Tkatchenko, P. Rodriguez-Lopez, A. W. Rodriguez, and R. Podgornik, *Rev. Mod. Phys.* **88**, 045003 (2016).

[6] D. A. T. Somers, J. L. Garrett, K. J. Palm, and J. N. Munday, *Nature* **564**, 386–389 (2018).

[7] T. Inoue, M. De Zoysa, T. Asano, and S. Noda, *Nat. Mater.* **13**, 928 (2014).

[8] J. W. Schwede, I. Bargatin, D. C. Riley, B. E. Hardin, S. J. Rosenthal, Y. Sun, F. Schmitt, P. Pianetta, R. T. Howe, Z.-X. Shen, and N. A. Melosh, *Nat. Mater.* **9**, 762 (2009).

[9] W. A. Challener, C. Peng, A. V. Itagi, D. Karns, W. Peng, Y. Peng, X. Yang, X. Zhu, N. J. Gokemeijer, Y.-T. Hsia, G. Ju, R. E. Rottmayer, M. A. Seigler, and E. C. Gage, *Nat. Photonics* **3**, 220 (2009).

[10] M. Krüger, G. Bimonte, T. Emig, and M. Kardar, *Phys. Rev. B* **86**, 115423 (2012).

[11] M. Krüger, T. Emig, G. Bimonte, and M. Kardar, *EPL* **95**, 21002 (2011).

[12] M. Katoh, M. Fujimoto, H. Kawaguchi, K. Tsuchiya, K. Ohmi, T. Kaneyasu, Y. Taira, M. Hosaka, A. Mochihashi, and Y. Takashima, *Phys. Rev. Lett.* **118**, 094801 (2017).

[13] M. F. Maghrebi, A. V. Gorshkov, and J. D. Sau, *Phys. Rev. Lett.* **123**, 055901 (2019).

[14] K. Y. Bliokh, J. Dressel, and F. Nori, *New J. Phys.* **16**, 093037 (2014).

[15] M. Durach and N. Noginova, *Phys. Rev. B* **96**, 195411 (2017).

[16] A. Mock, D. Sounas, and A. Alù, *Phys. Rev. Lett.* **121**, 103901 (2018).

[17] M. L. N. Chen, L. J. Jiang, and W. E. I. Sha, *Appl. Sci.* **8** (2018).

[18] F. Bouchard, I. De Leon, S. A. Schulz, J. Upham, E. Karimi, and R. W. Boyd, *Appl. Phys. Lett.* **105**, 101905 (2014).

[19] E. Nagali, F. Sciarrino, F. De Martini, L. Marrucci, B. Piccirillo, E. Karimi, and E. Santamato, *Phys. Rev. Lett.* **103**, 013601 (2009).

[20] S. M. Rytov, Y. A. Kravtsov, and V. I. Tatarskii, *Principles of Statistical Radiophysics 3* (Springer, Berlin, 1989).

[21] D. Polder and M. Van Hove, *Phys. Rev. B* **4**, 3303 (1971).

[22] H. B. Callen and T. A. Welton, *Phys. Rev.* **83**, 34 (1951).

[23] G. Bimonte, T. Emig, M. Kardar, and M. Krüger, *Annu. Rev. Condens. Matter Phys.* **8**, 119 (2017).

[24] T. Zhu and J.-S. Wang, *Phys. Rev. B* **104**, L121409 (2021).

[25] P. R. Buerzli and P. A. Martin, *Phys. Rev. E* **77**, 011114 (2008).

[26] A. W. Rodriguez, O. Ilic, P. Bermel, I. Celanovic, J. D. Joannopoulos, M. Soljačić, and S. G. Johnson, *Phys. Rev. Lett.* **107**, 114302 (2011).

[27] M. T. H. Reid, A. W. Rodriguez, J. White, and S. G. Johnson, *Phys. Rev. Lett.* **103**, 040401 (2009).

[28] S. J. Rahi, T. Emig, N. Graham, R. L. Jaffe, and M. Kardar, *Phys. Rev. D* **80**, 085021 (2009).

[29] M. Krüger, T. Emig, and M. Kardar, *Phys. Rev. Lett.* **106**, 210404 (2011).

[30] R. Messina and M. Antezza, *Phys. Rev. A* **84**, 042102 (2011).

[31] X. Gao, C. Khandekar, Z. Jacob, and T. Li, *Phys. Rev. B* **103**, 125424 (2021).

[32] L. A. Falkovsky, *Journal of Physics: Conference Series* **129**, 012004 (2008).

[33] J.-S. Wang, J. Wang, and J. T. Lü, *Eur. Phys. J. B* **62**, 381 (2008).

[34] J.-S. Wang, B. K. Agarwalla, H. Li, and J. Thingna, *Front. Phys.* **9**, 673 (2014).

[35] See supplementary materials for details on NEGF notations, derivation of the Meir-Wingreen formulas, discussion on bath at infinity, derivation of formulas in the eigenmode representation, definitions of velocity matrix, and density plot of radiations from zigzag and armchair graphene edges.

[36] W. Heisenberg and W. Pauli, *Z. Phys.* **59**, 168 (1930).

[37] D. C. Langreth, in *Linear and Nonlinear Electron Transport in Solids*, edited by J. T. Devreese and V. E. van Doren (Springer, Boston, MA, 1976).

[38] T. Zhu, M. Antezza, and J.-S. Wang, *Phys. Rev. B* **103**, 125421 (2021).

[39] J. Peng, H. H. Yap, G. Zhang, and J.-S. Wang, A scalar photon theory for near-field radiative heat transfer (2017), arXiv:1703.07113 [cond-mat.mes-hall].

[40] Z.-Q. Zhang, J.-T. Lü, and J.-S. Wang, *Phys. Rev. B* **101**, 161406 (2020).

[41] S. Datta, *Electronic Transport in Mesoscopic Systems* (Cambridge University Press, Cambridge, 1995).

[42] O. V. Kibis, M. Rosenau da Costa, and M. E. Portnoi, *Nano Letters* **7**, 3414 (2007).

[43] M. Freitag, H.-Y. Chiu, M. Steiner, V. Perebeinos, and P. Avouris, *Nat. Nanotech.* **5**, 497 (2010).

[44] R. R. Nair, P. Blake, A. N. Grigorenko, K. S. Novoselov, T. J. Booth, T. Stauber, N. M. Peres, and A. K. Geim, *Science* **320**, 1308 (2008).

[45] B. Müller and M. Krüger, *Phys. Rev. A* **93**, 032511 (2016).

[46] K. Wakabayashi, K. ichi Sasaki, T. Nakanishi, and T. Enoki, *Sci. Technol. Adv. Mater.* **11**, 054504 (2010).